Novel GaAs and Silicon Sensor Planes for Compact Sampling Calorimeters

H. Abramowich[1], Y. Benhammou[1], W. Daniluk[2], M. Firlej[2], T. Fiutowski[2], V. Ghenescu[3], M. Idzik[2], J. Kotula[2], A. Levy[1], I. Levy[1], W. Lohmann[4,5*], J. Moron[2], A. T. Neagu[3], M. Potlog[3] and K. Swientek[2]

[1]Raymond & Beverly Sackler School of Physics & Astronomy, Tel Aviv University, Tel Aviv, 610101, Israel.
[2]Faculty of Physics and Applied Computer Science, AGH University of Science and Technology, Krakow,Poland.
[3]Institute of Space Science, Bucharest, 077125, Romania.
[4]Deutsches Elektronen Synchrotron, PLatanenallee 6, Zeuthen, 15754, Germany.
[5]Institut for Compututional Physics, Brandenburg University of Technologhy, Platz der Deutschen Einheit 1, Cottbus, 03046, , Germany.

*Corresponding author(s). E-mail(s): wlo@ifh.de;

Abstract

Two samples of silicon pad sensors and two samples of GaAs sensors are studied in an electron beam of 5 GeV. The sensor size is 5x8 cm^2, the thickness 320 μm and 500 μm for the silicon and GaAs sensors, respectively. The pad size is 5x5 mm^2. The sensors are foreseen to be used in a compact electromagnetic sampling calorimeter. Therefore the readout of the pads is done via traces connected to the pads and to bond pads at the edges of the sensors. For the silicon sensors copper traces on a Kapton foil are used, connected to the sensor pads with conducting glue. The pads of the GaAs sensors are connected to the bond pads via aluminum traces on the sensor substrate. For the read out Flame front-end pre-amplifiers and ADCs are used. Pre-processing of the raw data and deconvolution is performed with FPGAs. The whole system is orchestrated by a Trigger Logic Unit TLU. Results are shown for the homogeneity of the response, edge effects at pads and sensors, and cross talk due to the readout traces.

Keywords: silicon pad sensors, GaAs pad sensors, Flame FE electronics, compact electromagnetic calorimeters

1 Introduction

For several applications of electromagnetic calorimeters the Moliere radius is a relevant parameter. Examples are luminometers in experiments at electron-positron colliders and an ECAL in laser-electron scattering. In the former Bhabha scattering is used as a gauge process. Using a highly compact calorimeter, i.e. with a small Moliere radius, the fiducial volume is well defined, and the space needed is relatively small. In addition, the measurement of the shower of a high energy electron on top of widely spread low energy background is facilitated. In the latter the number of electrons per bunch crossing varies over a wide range, and both the determination of the number of electrons and their energy spectrum per bunch crossing favours a highly compact calorimeter. In sampling calorimters as absorber material tungsten is chosen, with an Moliere radius of about 9.3 mm. Tungsten plates are interspersed with GaAs or silicon pad sensors to form a sandwich. To keep the Moliere radius near the one of tungsten, the gap between tungsten plates must be kept small. Hence thin sensor planes are needed. Two technologies are applied. In both thin metal traces guide the signal to the sensor edge where the FE ASICs are positioned. For GaAs sensor, these traces are made of aluminum, embedded in the gaps between the pads, and for silicon sensors Kapton fan-outs with copper traces are used.

2 Sensors

Silicon sensors, produced by Hamamatsu, are arrays of $5.5 \times 5.5 mm^2$, $p+$ on n substrate diodes. The thickness is $320 mum$ and the resistivity $3 k\Omega cm$, and the reverse bias voltage about $100 V$. Each sensor has a total area of $89.9 \times 89.9 mm^2$, structured in 16×16 pads, without guard ring. A picture of a sensor is shown in Fig. 1.

For all pads of the two sensors studied the leakage current was measured as a function of the bias voltage. A typical result is shown in Fig. 2. In order to route the signal from the pads to the front-end board, a Kapton PCB has been used. It is glued on the silicon sensors with a conductive glue. Another Kapton PCB has been produced to connect the bias voltage to the sensor back-plane.

GaAs sensors are made of single crystals. High resistivity of $10^9\,\Omega$m is reached by compensation with chromium. The pads are $4.7 \times 4.7\,\mathrm{mm}^2$, with 0.3 mm gap between pads. Pads consist of a $0.05\,\mu$m vanadium layer, covered with a $1\,\mu$m aluminium, made with electron beam evaporation and magnetron sputtering. The back-plane is made of nickel and aluminium of 0.02 and $1\,\mu$m thickness, respectively. The sensors are $550\,\mu$m thick with overall sizes of $51.9 \times 75.6\,\mathrm{mm}^2$. The active area is $74.7 \times 49.7\,\mathrm{mm}^2$ leading to 15×10 pads without

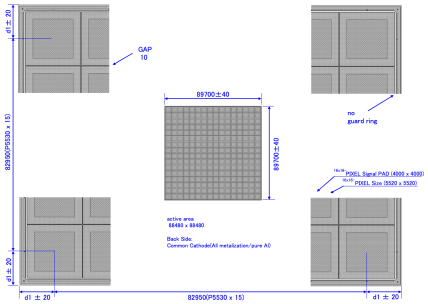

Fig. 1 Details of the geometry of the silicon sensor.

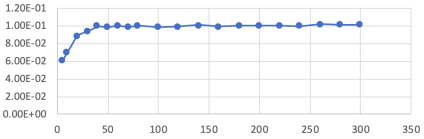

Fig. 2 Leakage current (in nA) as a function of the applied voltage (in V) for a selected pad.

guard rings. The signals from the pads are routed to bond pads on the top edge of the sensor by aluminium traces implemented on the sensor itself, thus avoiding the presence of a flexible PCB fanout. The traces are made of 1 μm thick aluminium film deposited on the silicon dioxide passivation layer by means of magnetron sputtering. A prototype sensor is shown in Fig. 3.

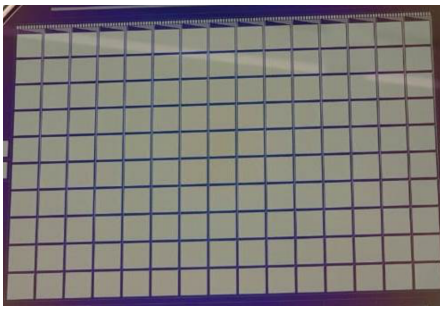

Fig. 3 Picture of a GaAs sensor. The bond pads are visible on top of the sensor.

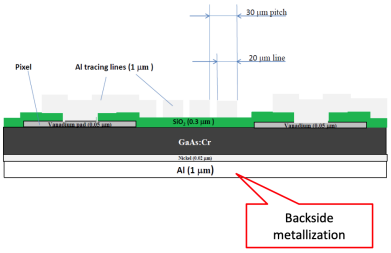

Fig. 4 Cross-profile of a GaAs sensor. The aluminium traces are positioned between the pads, on the top of the passivation layer.

Details on the sensor structure can be seen in the cross-profile shown in Fig. 4. Using several prototype sensors, the leakage current of all pads was measured as a function of the bias voltage. A typical example is shown in Fig. 5. At a bias voltage of 100 V the leakage current amounts to about 50 nA.

The implementation of the aluminium traces is a new technology, and its performance with respect to cross-talk and noise is presented below.

3 Front-End Electronics and Data Acquisition

Each sensor plane is read out by FE ASICs called FLAME (**F**ca**L** **A**sic for **M**ultiplane r**E**adout), designed for silicon-pad detectors of the LumiCal calorimeter for a future electron-positron linear collider experiment. The main

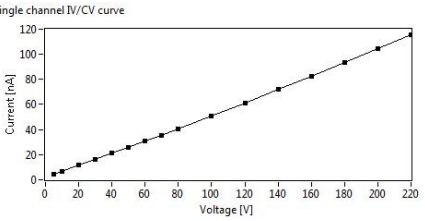

Fig. 5 The leakage current of a pad as a function of the bias voltage, measured at 20°C.

specifications of the FLAME ASIC are shown in Table 1. A block diagram

Variable	Specification
Technology	TSMC CMOS 130 nm
Channels per ASIC	32
Power dissipation/channel	$\sim 2\ mW$
Noise	$\sim$1000 e^-@10 pF + 50e^-/pF
Dynamic range	Input charge up to $\sim 6pC$
Linearity	Within 5% over dynamic range
Pulse shape	T_{peak} ~55 ns
ADC bits	10 bits
ADC sampling rate	up to $\sim 20\ MSps$
Calibration modes	Analogue test pulses, digital data loading
Output serialiser	serial Gb-link, up to 9 GBit/s
Slow controls interface	I^2C, interface single-ended

Table 1 Summary of the specifications of the FLAME ASIC.

of FLAME, a 32-channel ASIC designed in TSMC CMOS 130 nm technology, is shown in Fig. 6. FLAME comprises an analog front-end and a 10-bit ADC in each channel, followed by a fast data serialiser. It extracts, filters and digitises analogue signals from the sensor, performs fast serialisation and transmits serial output data. As seen in Fig. 6, the 32-channel chip is designed

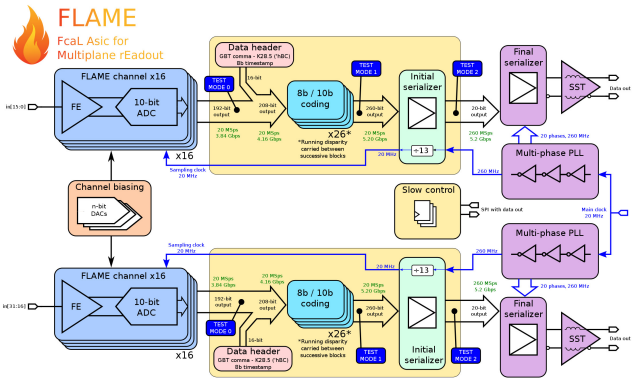

Fig. 6 Block diagram of a 32-channel FLAME ASIC

as a pair of two identical 16-channel blocks. Each block has its own serializer and data transmitter so that during operation two fast data streams are continuously sent to an external data acquisition system (DAQ). The biasing circuitry is common to the two 16-channel blocks and is placed in between. Also the slow control block is common and only one in the chip. The analogue front-end consists of a variable gain preamplifier with pole-zero cancellation (PZC) and a fully differential CR–RC shaper with peaking time ~ 55 ns. The shaper includes also an 8-bit DAC, with 32 mV range, for precise baseline setting. The analogue front-end consumes in total $1-1.5$ mW/channel. The ADC digitises with 10-bit resolution and at least 20 MSps sampling rate. The power consumption is below 0.5 mW per channel at 20 MSps. In order to ensure the linearity of the ADC, the input switches are bootstrapped, reducing significantly their dynamic resistance. The dynamic range of the ASICs can be switched between high and low gain. At high gain the response to the input charge is almost linear between deposition from 0.5 to 75 minimum-ionising-particle (MIP) equivalent. At low gain the charge at the preamplifier input is limited to 5 pC, corresponding to about 10000 MIP-equivalent, and the lower threshold is in the range of a few 10 MIP-equivalent.

The data from the ASICs are sent to the back-end FPGA board. A trigger signal will be sent to the FPGA, distributing it to the FLAME ASICs. Up to 128 raw ADC samples are collected in an event for each of the readout channels. In the raw data readout mode all ADC samples are recorded. In the standard readout mode the event is processed by the FPGA. For signals on pads above a predifined threshold the deposited charge and the Time Of Arrival, TOA, are calculated and recorded. This procedure, combined with zero suppression, significantly reduces amount of data. Finally, the event data are send from the FPGA board to the DAQ computer using the User Datagram Protocol, UDP, through a single 1 Gbps Ethernet link.

4 Beam, Trigger and Beam Telescope

Electrons of 5 GeVproduced in the DESY3 facility are used in this study. The electrons pass a collimator of 12 x 12 mm^2 aperture. Two scintillation counters up- and downstream of the beam telescope are used to form a trigger signal in the TLU. The beam telescope comprises 6 planes of Alpide sensors of a sensitive area of 1.5 cm x 3.0 cm and a pixel pitch of 29.24 μm x 26.88 μm. Just downstream of the last telescope plane the sensors are positioned. A sketch of the test beam set-up is shown in Fig. 7. Both the telescope sensors and the sensor under test are read out separately after arrival of a TLU trigger signal and form an event. The TLU delivers a trigger number for synchronising the records from the telescope and the sensor. In addition, a time stamp is given to each record. The trigger rate during data taking was about 1.5 kHz.

The beam telescope is used to measure the trajectory of each beam electron. For the alignment of the telescope planes and the track reconstruction the software package corryvrekan was used. For the alignment 50 k events at the

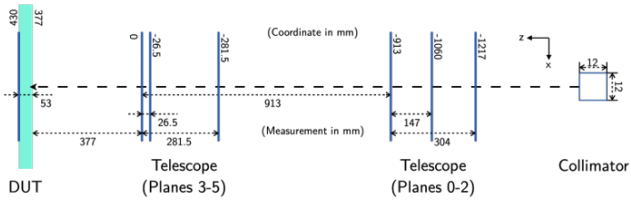

Fig. 7 Scheme of the test beam set-up. Electrons arrive from the right, pass the first scintillator, then six Alpide sensor plans, the second scintillator, and hit the sensor, denoted here as DUT (Detector under Test)

beginning of each run were used. A typical χ^2 distribution of the tack fit is shown in Fig. 8 The uncertainty of the prediction of the impact point of the

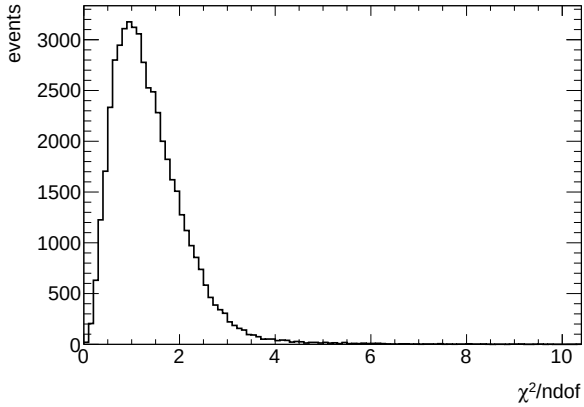

Fig. 8 χ^2/NDF distribution of electron trajectories fitted in the telescope.

electron on the sensor plane amounts 30 μm, dominated by multiple scattering in the downstream telescope plane.

5 Data

6 Results

6.1 Response on Single Pads

Here the response of single pads should be shown and discussed, signal distribution example, compared with the results from raw data, simulation, homogeneity of the response (MPV as function of pad number)

6.2 Low and High Gain Comparison

compare signal sizes when FE electronics is set to high and low gain

6.3 Effects Near the Edges of a Pad

Scanning the signal size as a function of the local coordinate between the edges

6.4 Cross Talk Between Pads

Acknowledgments. Acknowledgments are not compulsory. Where included they should be brief. Grant or contribution numbers may be acknowledged.

Please refer to Journal-level guidance for any specific requirements.

References